Experimental Determination of Conduction and Valence Bands of Semiconductor Nanoparticles using Kelvin Probe Force Microscopy

Wen Zhang and Yongsheng Chen

School of Civil and Environmental Engineering, Georgia Institute of Technology, Atlanta, Georgia, 30332, USA.
Email: yongsheng.chen@ce.gatech.edu; Phone: (+1) 404-894-3089; Fax: (+1) 404-894-2278.

ABSTRACT

The ability to predict a semiconductor's band edge positions in solution is important for the design of photocatalyst materials. In this paper, we introduce an experimental method based on Kelvin probe force microscopy (KPFM) to estimate the conduction and valence band edge energies of semiconductors, which has never been demonstrated experimentally. We test the method on six well known semiconductor materials: α-Fe_2O_3, CeO_2, Al_2O_3, CuO, TiO_2, and ZnO. The predicted band edge positions for α-Fe_2O_3, Al_2O_3, and CuO were not statistically different from the literature values. Except CeO_2, all other metal oxides had consistent upward bias in the experimental determination of band edge positions probably because of the potential shielding effect of the adsorbed surface water layer. This experimental approach represents a unique way of probing the band edge energy positions of metal oxide materials without using the thermodynamic information (e.g., enthalpy or entropy), which is often not available for new synthetic or complex materials.

Keywords: conduction band, valence band, water-splitting, photocatalyst, KPFM, work function

1 INTRODUCTION

Determination of the band gaps (E_g), energy edge positions of conduction and valence bands (E_V and E_C) is critical for many photochemical processes (e.g., photocatalytic reactions for water-splitting) and the design of appropriate photocatalysts [1]. In particular, in a water-splitting reaction, photocatalyst materials must have a conduction-band minimum (CBM) more negative than the H_2O/H_2 level of water and a valence-band maximum (VBM) more positive than the H_2O/O_2 level of water, which ensures that the water-splitting reaction is energetically favorable (e.g., the reducing power of the photo-excited electrons in the conduction band can sufficiently reduce H^+ and generate H_2) [2]. Therefore, the knowledge of a semiconductor's CBM and VBM band edge positions is important for the design of photocatalysts.

Theoretical approaches for computing the band edge energies of CB and VB have been studied using density function theory (DFT) [1, 3]. However, such theoretical computation requires the crystallographic information of the photocatalysts such as the volume, cell shape, and atomic positions of the unit cell. Moreover, computational methods are limited to simple chemicals (e.g., binary oxides) with well-known thermodynamic data such as standard enthalpies of formation and standard free energies, which are not available for new synthetic materials or difficult to obtain [4]. Thus, the electrical and electronic characterization of photocatalysts can be challenging, due to the complexity of their compositions, chemical structures, and the presence of defects. A straightforward attempt for this purpose is to develop experimental methods that are easily operated on any unknown materials.

Kelvin probe force microscopy (KPFM) is a useful tool that has been demostrated in nanometer-scale imaging and quantification of the surface potential on a broad range of materials [5, 6]. KPFM provides a noncontact and noninvasive mapping of the local surface potential, which is the contact potential differences (CPD) due to the difference in work functions (or Fermi energy levels) between the sample surface and the tip. Work function, usually measured in eV, is the energy difference of an electron between the vacuum level and is equal to the Fermi level, which is the minimum energy needed to liberate an electron from the surface of semiconductors [6, 7]. The local mechanical and electromagnetic properties, such as surface charges, doping levels, or dielectric constants, significantly affect the work function. Thus, KPFM can be used to study defects or grain boundaries and to quantify the surface work function on single crystallographic planes [8]. In addition, KPFM has applications in the development of devices such as laser diodes or photovoltaic (PV) solar cells to probe the surface electronic states. As the striking advantage of AFM-based scanning probe systems, KPFM is suitable for investigating a variety of materials, from metallic to metal oxides and organics [9, 10].

In this study, the determination of the work function of different metal oxide nanomaterials on a local scale was obtained by KPFM. The CB and VB edge energy positions of sixe types of oxide nanoparticles (α-Fe_2O_3, CeO_2, Al_2O_3, CuO, TiO_2, and ZnO), were then calculated with the relationship between band edge energies and work function (to be introduced below). Finally, we compare the experimental results to literature values.

2 EXPERIMENTAL SECTION

All metal-oxide nanoparticles were purchased from Sigma-Aldrich, except TiO_2 was purchased from Degussa, Al_2O_3 from Nanostructured & Amorphous Materials. Particles were visually examined by a Philips EM420 transmission electron microscope (TEM) operating in a bright field mode at an acceleration voltage of 28–47 kV. Table 1 summarizes the details of the nominal particle sizes, purity, and electronic properties. KPFM was performed on the Agilent 5500 AFM with the detailed procedures described previously [9]. Briefly, Pt-coated silicon cantilever probes (Olympus AC240TM, Japan) were used as the conductive probes with a force constant of approximately 2–5 N/m and a nominal resonance frequency of 70 kHz. Nanoparticles were immobilized on undoped (100) silicon wafer (Sigma-Aldrich) by depositing 2.5−μL water suspensions with for approximately 5-min air drying. During the operation, the microscope was fully contained in an environmental chamber that controls ambient pressure, temperature (25 ± 2°C), and humidity (approximately 35%) as measured by a VWR® humidity/temperature thermometer).

Since CPD= φ_{tip}-φ_{sample} [11], the work function of the sample (φ_{sample}) can be obtained (φ_{sample}= φ_{tip} –CPD_{sample}), once the work functions of the Pt/Au conductive tip (φ_{tip}) is determined. φ_{tip} was calibrated with freshly cleaved highly oriented pyrolytic graphite (HOPG grade ZYH, Product No. 626, Ted Pella, USA), knowing that CPD_{HOPG}=φ_{tip}-φ_{HOPG}, where the work function of HOPG (φ_{HOPG}) in air is 4.65 eV [7, 12] and CPD_{HOPG} is the CPD measured on the HOPG sample surface. The absolute surface work function of the Pt-coated conductive cantilever probes (φ_{tip}) is 4.91±0.05 eV (averaged from 6 different cantilevers). In principle, each cantilever tip we used shall go through the calibration to determine individual work function. However, to avoid the tip contamination or damage, we calibrated two or three tips from each batch of cantilevers that generally exhibit the same surface electronic properties.

For an undoped intrinsic oxide, the surface work function or Fermi level, E_F, is the nergy level at which the probability of occupation by an electron is ½ and lies at the mid-point of the band gap. Thus, CBM and VBM are related to the sample work function [13, 14]:

$$E_C=-\varphi_{sample}+0.5E_g \quad (1)$$

$$E_V=-\varphi_{sample}-0.5E_g \quad (2)$$

where E_C is CBM, E_V is VBM, and E_g is the band gap.

Table 1. Properties of the selected metal oxides.

	Particle diameter (nm)	Purity (%)	E_g (eV)*	E_C (eV)	E_V (eV)	Ref.
α-Fe_2O_3	50	99.0	2.20	-4.78	-6.98	[15]
CeO_2	25	99.95	3.30	-2.70	-6.00	[16, 17]
Al_2O_3	10-25	99.97	8.53	-1.32	-9.85	[14]
CuO	50	99.9	1.70	-4.96	-6.66	[15]
TiO_2	25	99.70	3.20	-4.21	-7.41	[15]
ZnO	50	99.9	3.20	-4.19	-7.39	[15][18]

*Literature values of band gap, E_C and E_V are for 25 °C with respect to the absolute vacuum scale (AVS).

3 RESULTS AND DISCUSSION

Fig. 1 shows the TEM images of six different metal oxide nanoparticles, most of which appear to be in particle-shape or aggregated clusters, except that Al_2O_3 was amorphous. The KPFM images in the middle column deliver the information of both particle morphogy and local surface potentials. The particle shape and size were generally consistent with TEM images. For instance, α-Fe_2O_3 had the identital spherical shape in both TEM and KPFM images. The precise measurement of surface potential or CPD is achieved by drawing a red dotted line across the particles of interest in the surface potential images, which results in the cross-sectional profiles shown in the right column. The statistical measurements of CPD values for different metal oxides are shown in the cross-sectional profiles. As mentioned above, the absolute work function of each metal oxides (φ_{sample}) can be calculated. For example, knowing Φ_t=4.91±0.05 eV and CPD for α-Fe_2O_3 is approximately -800 mV (mean), we can determine φ_{sample}.of α-Fe_2O_3 to be 5.71±0.20 eV, which agreed well with the literature value [13]. Finally, according to Eqs. (1) and (2), E_C and E_V were obtained with E_F replaced by φ_{sample}.for different metal oxides.

Fig. 2 compares the literature reported values of CB and VB and our experimental data, which for most oxides well match the literature values with the similar upward bias, except CeO_2. Experimental results of E_C and E_V appeared slightly lower in magnitude than literature values, probably because the moisture or water adsorption on the sample surface resulted in a potential shielding effect of the adsorbed water layer as indicated previously [7, 15]. The opposite downward bias in the positions of CB and VB could reflects the direction and amount of band bending caused by other surface states (e.g., hydrophobicity and surface charge) in addition to the surface moisture content [15].

It is worth mentioning that Fig. 2 presents the electronic properties of the bulk scale metal oxides without considering the potential size effect on E_g or the band edge positions [16]. The electronic structures of small nanoparticles (less than 10 nm) are probably different from those of bulk materials owing to quantum confinement effects. For instance, small nanoparticles likely have larger E_g values than their bulk counterparts, and their band edge positions shift with respect to the positions of bulk materials. However, nanoparticles used in our study have diameters of 25–50 nm; such NPs have bulk-like electronic structures [14], and thus changes in electronic structure should not cause the differences in the photochemical properties of the tested NPs and their bulk counterpart.

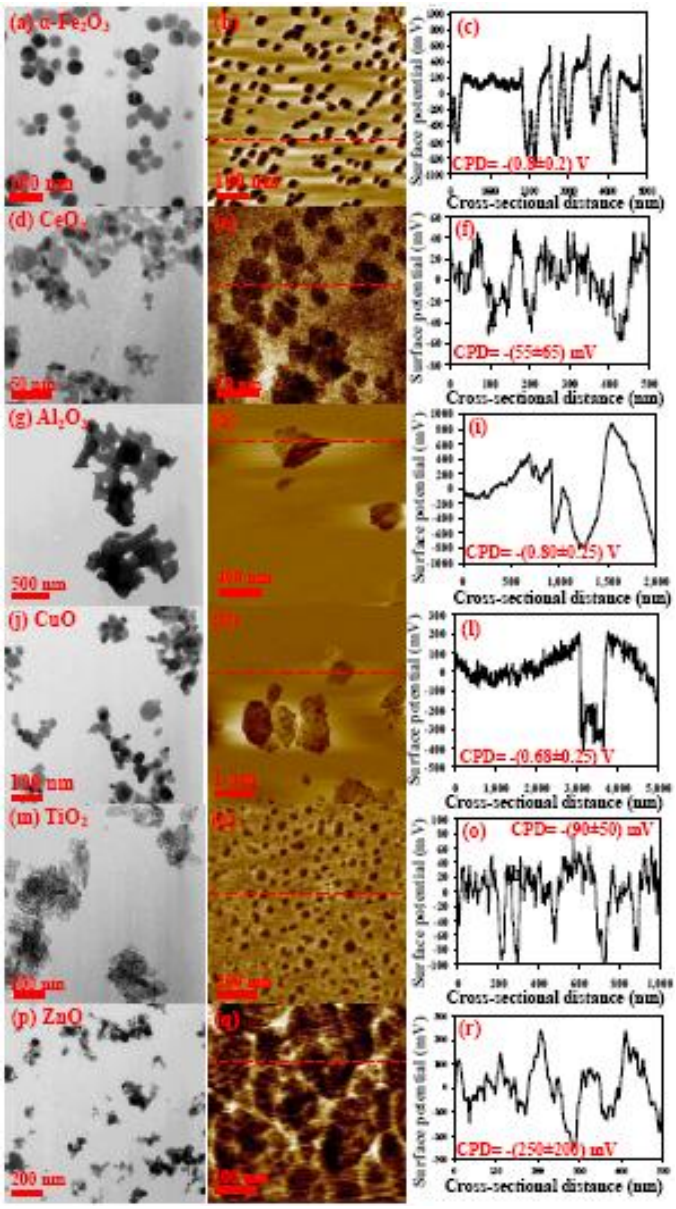

Figure 1. TEM images (the left column), surface potential images obtained from KPFM (the middle column), and the cross-sectional profiles of the surface potentials taken along the directions marked with the red dashed lines in the surface potential images. The measured CPD values for each type of metal oxide nanoparticles are shown in the cross-sectional profiles (expressed as the mean and standard deviations). Statistical analysis on the measurement of work function for each type of metal oxides were performed on at least 30 particles observed in each surface potential image.

This experimental approach represents a unique way of estimating the band edge positions or E_C and E_V of metal oxide materials. In contrast, conventional methods for the determination of E_V and E_C are based on theoretical calculations (e. g., DFT) are confined to the simple materials (e.g., diatomic compounds) and often requires the thermodynamic information of enthalpy or entropy, which is unavailable or difficult to estimate for new nanomaterials. One may argue that the calculation in Eqs. (1) and (2) relies on the information of band gap (E_g), which may not be available for unknown materials. However, it is noted that the band gap of a material can be determined by UV–VIS diffuse reflectance spectroscop [17], which is essentially allows us to characterize the band gaps of any unknown materials.

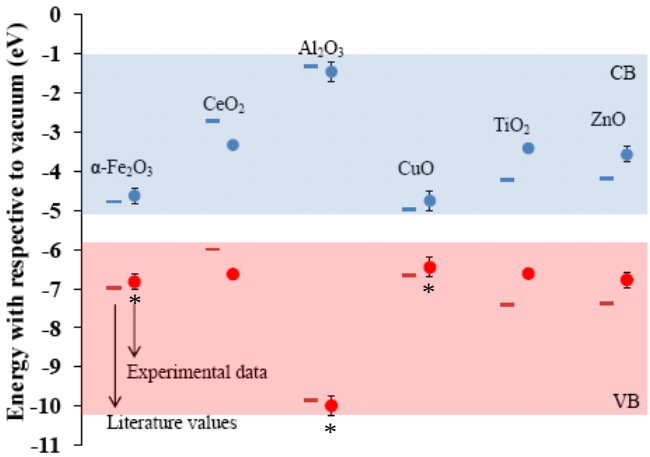

Figure 2. Comparison between the literature values (bar data) and experimental values (dot data) of CB and VB positionsfor selected metal oxide semiconductors with respect to absolute vacuum scale (AVS). Blue and red colored data represent CBM and VBM, respectively, while the blue shaded area represents the conduction band (*E*c), while the red shaded area represents the valence band (*E*v), respectively. Error bars for the dot data indicate the standard deviations. When not visible, error bars are smaller than the size of the symbol. * indicates no statistical difference between experimental and literature values (p<0.05, n=50).

4 CONCLUSION

Simultaneous mapping of topography and surface potential (or work function) positions KPFM as a unique tool to characterize the electrical properties of oxide materials, which are of importance for many applications in materials science and nanotechnology. In this study, KPFM was successfully demostrated to measure the work function of six different metal oxide nanoparticles and the conversion of the work function using Eqs. (1) and (2) allows us to estimate the band energy edge positions (CB and VB). The predicted band edge positions for α-Fe_2O_3, Al_2O_3, and CuO were in good agreement with the literature values, whereas other metal oxides (TiO_2 and ZnO) except CeO_2 had similar upward bias (or lower in magnitude for the band edge energies) in the experimental determination compared to the literature values, probably because of the potential shielding effect of the adsorbed surface water layer. The overall consitency or low errors in prediction of E_C and E_V for the six metal oxides make useful for predicting electronic structures and designing metal oxide materials. Moreover, KPFM is suitable for investigating a

wide variety of materials at different scales, particularly ideal for probing nanostructures for electronic properties.

5 REFERENCES

[1] Y.B. Wu, M.K.Y. Chan, G. Ceder, Prediction of semiconductor band edge positions in aqueous environments from first principles, Physical Review B 83 (2011).

[2] M. Gratzel, Photoelectrochemical cells, Nature 414 (2001) 338-344.

[3] A. Filippo De, F. Simona, S. Annabella, Alignment of the dye's molecular levels with the TiO_2 band edges in dye-sensitized solar cells: a DFT–TDDFT study, Nanotechnology 19 (2008) 424002.

[4] J. Portier, H.S. Hilal, I. Saadeddin, S.J. Hwang, M.A. Subramanian, G. Campet, Thermodynamiccorrelations and bandgap calculations in metal oxides, 32 3-4 (20047).

[5] W. Melitz, J. Shen, A.C. Kummel, S. Lee, Kelvin probe force microscopy and its application, Surface Science Reports 66 (2011) 1-27.

[6] R. Berger, H.-J. Butt, M.B. Retschke, S.A.L. Weber, Electrical modes in scanning probe microscopy, Macromol. Rapid Commun. 30 (2009) 1167-1178.

[7] A. Liscio, V. Palermo, K. Mullen, P. Samori, Tip-sample interactions in Kelvin probe force microscopy: quantitative measurement of the local surface potential, J. Phys. Chem. C 112 (2008) 17368-17377.

[8] T. Glatzel, S. Sadewasser, R. Shikler, Y. Rosenwaks, M.C. Lux-Steiner, Kelvin probe force microscopy on III-V semiconductors: the effect of surface defects on the local work function, Materials Science and Engineering B-Solid State Materials for Advanced Technology 102 (2003) 138-142.

[9] W. Zhang, Y. Yao, Y. Chen, Imaging and quantifying the morphology and nanoelectrical properties of quantum dot nanoparticles interacting with DNA, J. Phys. Chem. C 115 (2011) 599–606.

[10] L. Sun, J.J. Wang, E. Bonaccurso, Nanoelectronic properties of a model system and of a conjugated polymer: a study by Kelvin probe force microscopy and scanning conductive torsion mode microscopy, J. Phys. Chem. C 114 (2010) 7161-7168.

[11] R.F. Gouveia, F. Galembeck, Electrostatic charging of hydrophilic particles due to water adsorption, J. Am. Chem. Soc. 131 (2009) 11381-11386.

[12] A. Liscio, V. Palermo, P. Samorì, Nanoscale quantitative measurement of the potential of charged nanostructures by electrostatic and Kelvin probe force microscopy: unraveling electronic processes in complex materials, Acc. Chem. Res. 43 (2010) 541-550.

[13] Y. Xu, M.A.A. Schoonen, The absolute energy positions of conduction and valence bands of selected semiconducting minerals, Am. Mineral. 85 (2000) 543-556.

[14] E. Burello, A.P. Worth, A theoretical framework for predicting the oxidative stress potential of oxide nanoparticles, Nanotoxicology 5 (2011) 228-235.

[15] H. Sugimura, Y. Ishida, K. Hayashi, O. Takai, N. Nakagiri, Potential shielding by the surface water layer in Kelvin probe force microscopy, Appl. Phys. Lett. 80 (2002) 1459-1461.

[16] N. Satoh, T. Nakashima, K. Kamikura, K. Yamamoto, Quantum size effect in TiO_2 nanoparticles prepared by finely controlled metal assembly on dendrimer templates, Nature Nanotechnology 3 (2008) 106-111.

[17] C. Wang, J.C. Zhao, X.M. Wang, B.X. Mai, G.Y. Sheng, P. Peng, J.M. Fu, Preparation, characterization and photocatalytic activity of nano-sized ZnO/SnO2 coupled photocatalysts, Applied Catalysis B-Environmental 39 (2002) 269-279.